Journal of Mining and Metallurgy, 43 B (2007) 57 - 70

STUDY OF INITIAL STAGE OF MECHANOCHEMICAL TRANSFORMATION IN PYRITE

D. Paneva*, D. Mitova, E. Manova, H. Kolev, B. Kunev and I. Mitov

Institute of Catalysis, Bulgarian Academy of Sciences,
"Acad. G. Bonchev" Str., bl. 11, 1113 Sofia, Bulgaria

(Received 18 February 2007; accepted 19 July 2007)

Abstract

The initial stage of transformation of pyrite to Fe(II)-sulfate as a result of mechanical milling is studied by X-ray powder diffraction (XRD), Moessbauer spectroscopy (MS), Infrared (IR) and X-ray photoelectron spectroscopy (XPS) techniques. A degree of conversion of 0.071 is achieved in the time interval of 0-36 min. The kinetic data satisfy the equation of a shrinking core reaction $1-(1-\alpha)^{1/3}=kt$. The reaction is of the first order. The calculated rate constant is $k=6.434.10^{-4}$ min^{-1}.

Keywords: minerals, mechanochemistrty, pyrite oxidation, kinetics, Moessbauer spectroscopy.

1. Introduction

Pyrite (FeS2) is the most common sulfide mineral found in the earth's crust. When exposed to oxygen and water it is oxidized according to the following reaction [1,2]:

$$FeS_2 + 7/2\ O_2 + H_2O \rightarrow Fe^{2+} + 2\ SO_4^{2-} + 2\ H^+$$

[#] ***Corresponding author:*** daniela@ic.bas.bg
doi:10.2298/JMMB0701057P

Oxidation of pyrite is important in the geochemical and biogeochemical processes such as the cycling of S, Fe, and other elements in the environment [3, 4]. It has been shown that the important parameters affecting the pyrite oxidation are: pH [5, 6], concentration of oxygen, presence of bacteria [7-11], concentration of ferric ion [12], temperature [13], specific surface area of the mineral [14] and the trace metal content [15, 16].

Oxidation/reduction reactions have been shown to occur at room temperature in the course of mechanical milling. The mechanical activation of minerals is very important in different fields of solid processing technology. Mechanochemical activation refers to processes that increase the surface area. As the oxidation of pyrite is either directly (by oxygen) or indirectly (by ferric ion) driven by the accessibility of oxygen to sulfide surface, the increase of the surface could facilitate oxidation [17]. When the pyrite is mechanochemically treated in a high energy mill, the $FeS_2 \rightarrow FeSO_4 \cdot H_2O$ transformation [18] is associated with mechanochemical treatment. Pyrite is the most common sulfide host for gold and in refractory pyrite samples gold is encapsulated in the pyrite matrix, so this matrix must be broken down prior to cyanidation. According to reference [19] the mechanical treatment of pyrite yields fine particles of high porosity. The latter exert better reactivuty to cyanide used for the extraction of gold. The application [20] of mechanical activation of sulfides by intensive grinding in air changes their surface composition. The ratio between S^{2-} and S^{6+} species depends on the degree of mechanochemical surface oxidation.

Pyrite can be mechanochemically oxidized, with the sulfur retained as a sulfate without the production of sulfur dioxide gas. Potential exists for this process to form the basis for an economically viable, environmentally friendly process for the treatment of refractory pyritic gold ores. The aim of the present paper is to study the initial stage of iron sulfide to iron sulfate transformation using spectral methods.

2. Experimental

The pyrite concentrate of Bulgarian origin (Chelopech Co. Ltd) was investigated.

The mechanical activation was carried out in mill "VIVMP" (Russia) with

a rotating magnetic field. The mill had a diameter of 82 mm and a length of 160 mm. The diameter, length and weight of the milling bodies were 2.4 mm, 24 mm and 440 g, respectively. Magnetic induction was 0.168 T and synchronous part of bipolar magnetic field rotation - 3000 min^{-1}. Activation was performed in air. The time of mechanical treatment was varied from 6 to 36 min.

X-ray diffraction measurements were carried out on a TUR-M62 apparatus (Germany) equipped with a computer-controlled HZG-4 goniometer with Co-K radiation. The phase composition was identified according to JCPDS database [21].

Moessbauer spectra were obtained at room temperature with a Wissel (Wissenschaftliche Elektronik GmbH, Germany) electromechanical spectrometer working in a constant acceleration mode. A ^{57}Co/Cr (activity ≅ 10 mCi) source and an α-Fe standard were used. The experimentally obtained spectra were fitted to mathematical processing according to the least squares method. The parameters of hyperfine interaction such as isomer shift (IS), quadrupole splitting (QS) and effective internal magnetic field (H_{eff}) as well as the line widths (FWHM) and the relative weight (G) of the partial components of the spectra were determined.

The XPS measurements were carried out in the UHV chamber of a ESCALAB-MkII (VG Scientific, UK) electron spectrometer with a base pressure of 1.10^{-8} Pa. The photoelectron spectra were excited using unmonochromatized AlKα radiation (hν =1486.6 eV) with a total instrumental resolution of ~1 eV. The C1s, O1s, Fe2p, S2p, Si2p and Al2p photoelectron lines were measured. All spectra were calibrated by the C1s of adventitious carbon at 285 eV as a reference.

Infrared (IR) spectra of the samples were registered using the KBr pellet technique in the range 4000 - 300 cm^{-1} on a Nicolet 20SXC spectrometer.

3. Results and discussions

The diffraction patterns of non-activated pyrite and mechanochemically treated pyrite (36-min treatment) are shown on Fig.1. According to X-ray diffraction data the main phase component in the concentrate (non-activated sample) is pyrite (FeS_2, PDF 42-1340). The relatively low content of SiO_2

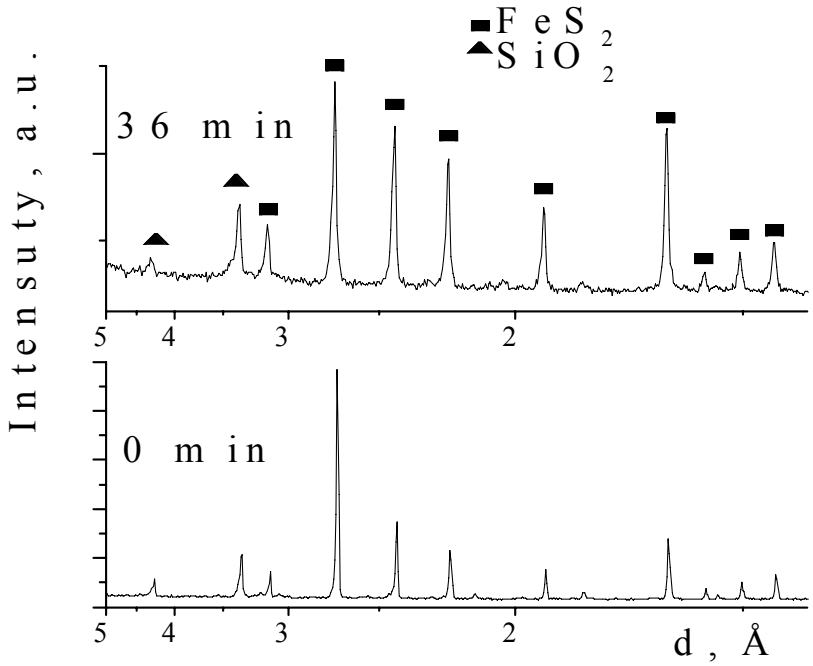

Fig. 1. XRD of non-activated and activated (36 min) samples

(PDF 83-2465) and trace of Al_2O_3 (PDF 83-2080) were determined. The phase composition of the mechanochemically treated sample includes a small amount of $FeSO_4 \cdot H_2O$ (PDF 45-1365). Little changes of phase composition indicate the strength of the covalent chemical bond in FeS_2. It depends on overlapping of the hybridized atomic orbitals: the $3d^2 4s 4p^3$ octahedral orbital of iron ion and the sp^3 tetrahedral orbital of the sulfur ion [22].

The effect of mechanical treatment reflects on the broadening and relatively less intensive lines in the diffraction spectrum of the activated sample. The changes observed in the spectrum of mechanoactivated sample are associated with the size of pyrite crystallite (D) and with the increased structural defects (E - degree of microstrain). A convolution model for D and E determination from diffraction line broadening was used with Voigt function as Profile function. The assignment of the Lorentzian component of a reflection is due to the grain size and that of its Gaussian component to the

strain distribution. The average crystallite size of the non-activated samples (0 min) and of the activated one (36 min) are D=113 nm and D=39 nm, respectively. The higher values of degree of microstrain for the activated sample ($E = 5{,}2 \cdot 10^3$, whereas $E = 4{,}5 \cdot 10^2$ at t=0 min) are associated with the fact that the mechanical treatment induces a gradual disordering of the crystal lattice and a consequent formation of an amorphous structure.

Changes in the pyrite crystal initiated by the mechanochemical treatment can be followed both by the Moessbauer spectra (Fig. 2) and by Moessbauer parameters (Table 1) of samples activated for different time. The spectrum of non-activated pyrite is a quadrupole doublet with IS=0.301 mm/s and QS=0.610 mm/s. These parameters coincide with that of the natural pyrite mineral [24]. The oxidation state of iron ions in pyrite is Fe^{2+}. They are octahedrally coordinated and in a low spin state. Data of Moessbauer spectroscopy measurements reveal that mechanochemical treatment of the solid causes a transition from a state with minimum energy to a new state with higher energy. The line broadening with increased time of mechanical treatment can be interpreted as an achievement of a set of various states of the iron atom, the latter being reported in the literature as a transition from a solid to a metastable state [18].

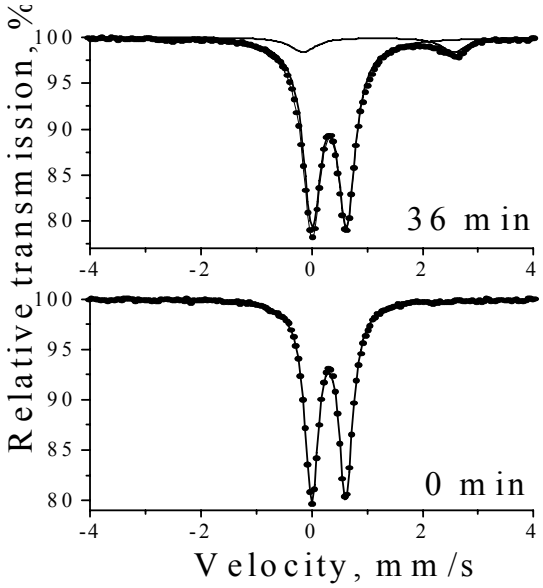

Fig. 2. Moessbauer spectra of non-activated and activated (36 min) samples

Two quadrupole doublets of Fe^{2+} are distinguished in the spectra of activated samples - one in a low (LS) and the second in a high spin (HS) state. In addition this treatment yields a partial transformation of Fe(II) sulfide to Fe(II) sulfate (~7.1 %). The values of the parameters of the second doublet in the Moessbauer spectra of samples activated for various time are approximately equal to the values corresponding to $FeSO_4 \cdot H_2O$ [18, 26, 27]. Moessbauer data reveal that the iron sulfate (szomolnokite) is formed at the first minutes. Subsequent treatment only increases its amount (Table 1).

Table 1. Moessbauer parameters of non-activated and activated samples

Milling time	Compounds	IS, mm/s	QS, mm/s	FWHM, mm/s	G, %
0 min	FeS_2	0.301	0.610	0.299	100
6 min	FeS_2	0.303	0.611	0.350	98.47
	$FeSO_4.H_2O$	1.280	2.710	0.350	1.53
12 min	FeS_2	0.308	0.612	0.375	96.70
	$FeSO_4.H_2O$	1.267	2.710	0.400	3.30
18 min	FeS_2	0.312	0.616	0.385	96.05
	$FeSO_4.H_2O$	1.286	2.711	0.439	3.95
24 min	FeS_2	0.315	0.619	0.394	94.66
	$FeSO_4.H_2O$	1.267	2.712	0.485	5.34
30 min	FeS_2	0.316	0.621	0.439	94.34
	$FeSO_4.H_2O$	1.278	2.711	0.420	5.66
36 min	FeS_2	0.317	0.626	0.454	92.84
	$FeSO_4.H_2O$	1.267	2.712	0.420	7.16

The kinetics of mechanochemical treatment is followed by the relative weights, G, of $FeSO_4 \cdot H_2O$ spectra. They were changed from 0 % (degree of transformation =0) to about 7.1 % (degree of transformation =0.071) after 36 minutes of mechanical treatment. The calculated values of degree of transformation are listed in Table 2.

Several equations for various models of solid state reactions [28, 29] have been tested to find the kinetic equation satisfying data in Table 2, namely:

Table 2. Values of α for samples activated during different time period

t, min	6	12	18	24	30	36
α	0.015276	0.032997	0.039466	0.053399	0.056556	0.071157

- Equation of Avrami-Erofeeff $-\ln(1-\alpha)^{1/n}=kt$ with n=1, 2, 3 and 4;
- Equation of Prout-Tompkins $\ln /(1-\alpha)=kt+C$;
- Shrinking area equation $1-(1-\alpha)^{1/2}=kt$;
- Shrinking core equation $1-(1-\alpha)^{1/3}=kt$;
- Equation of reaction order *n* with respect to transformation degree: $-\ln(1-\alpha)=kt$ for n=1 (the equation coincides with that of Avrami-Erofeeff for n=1), $(1-\alpha)^{-1}=kt$ for n=2 and $(1-\alpha)^{-2}=kt$ for n=3 ;
- Exponential equation for acceleration type reactions $\alpha^{1/n}=kt$ for n=1, 2, 3 and 4.

Figure 3 exhibits the relationships that do not satisfy experimental values - the plots are not linear. It should be noted that the values of G are rounded off. The plots concern the Avrami-Erofeeff equation for n=2, 3 and 4, equation of Prout-Tompkins and equation of a third order reaction.

Experimental data obtained fitted the following four equations, namely: shrinking core equation, shrinking area equation, Avrami- Erofeeff equation for n=1 (a first order reaction) and exponential equation for n=1. This is demonstrated on Fig. 4.

The values of the rate constant K (angle coefficient), the intersection on the ordinate b, dispersion of the points S_0^2, dispersion of the rate constant S_K^2 and the intersect S_b^2 are calculated using the least squares method. The results are summarized in Table 3.

The results of calculations reveal that the experimental data could be modeled by several kinetic equations. The most suitable one is selected based on detailed analysis.

The results of linearization using equation $-\ln(1-\alpha)=kt$ (equation of Avrami-Erofeeff for n=1 and equation of a first order reaction) unambiguously indicates that mechanical treatment runs according to a first order reaction.

It should be mentioned that different values for the rate constants are obtained applying different relationships (see Table 3). They differ to an order,

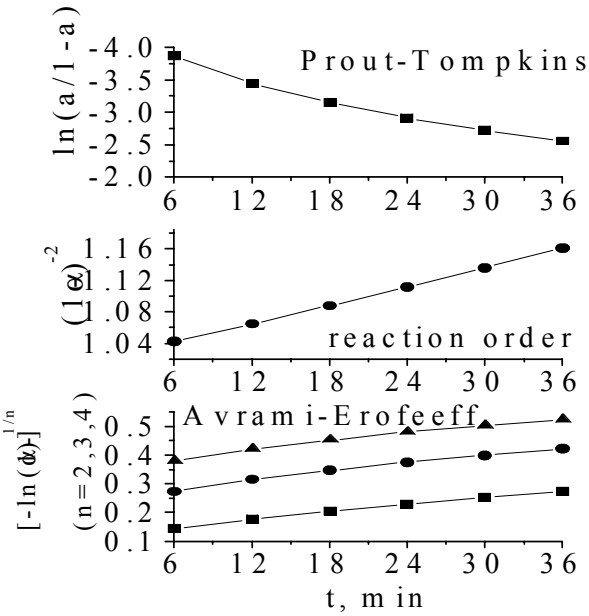

Fig 3. Relationships not satisfying experimental data

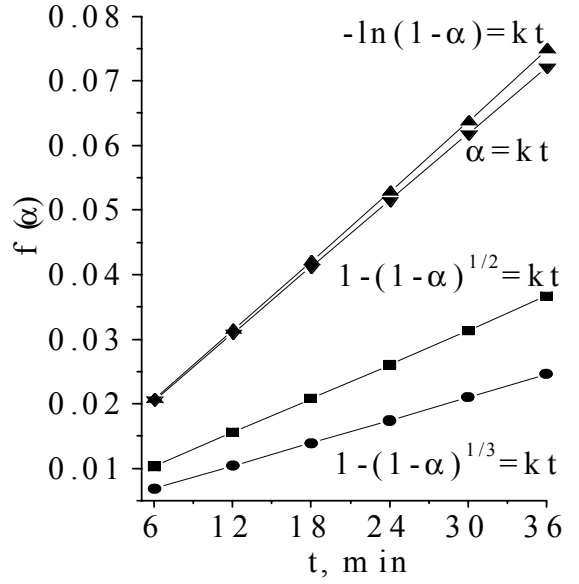

Fig. 4. Relationships, satisfying experimental data

Table 3. Kinetic data derived from the equations used

Magnitudes	Kinetic data			
	$\alpha=kt^{1/n}$ n=1	$-\ln(1-\alpha)^{1/n}=kt$ n=1	$1-(1-\alpha)^{1/2}=kt$	$1-(1-\alpha)^{1/3}=kt$
	Exponential law	Avrami-Erofeeff	Shrinking area	Shrinking core
Rate constant K, min^{-1}	$1,8835.10^{-3}$	$1,9558.10^{-3}$	$9,599.10^{-4}$	$6,434.10^{-4}$
Intersection on the ordinate b, $f(\alpha)$	$4,4815.10^{-3}$	$4,2596.10^{-3}$	$2,1927.10^{-3}$	$1,448.10^{-3}$
α ï ðè t=0	0,004815	0,0042505	0,0043806	0,004337
Dispersion of points, S_0^2	$1,82.10^{-5}$	$1,42.10^{-5}$	$4,40.10^{-6}$	$2,06.10^{-6}$
Dispersion of coefficient K, S_K^2	$1,805.10^{-8}$	$2,01.10^{-9}$	$4,36.10^{-9}$	$2,04.10^{-9}$
Dispersion of coefficient b, S_b^2	$8,45.10^{-6}$	$6,593.10^{-6}$	$2,043.10^{-6}$	$9,57.10^{-7}$

e.g. values calculated using the exponential law and the Avrami-Erofeeff equation on one side and that of shrinking area and shrinking core equations on the other. In this connection data representing the rate constants listed in Table 3 are of interest as comparable data.

In our case equation $\alpha=kt^{1/n}$ at n=1 is principally referred to reactions of accelerating type. Experimental data about degree of transformation reveal that the studied reaction does not belong to such type since it is monotonously increasing. We assume that this equation should be neglected. It is known [20], that the process of thermal transformation of FeS_2 to $FeS_{1.085}$ for $\alpha \cong 0.1$-0.9 obeys the shrinking core equation. The latter equation is applicable to particles with spherical shape and to crystal substances of a cubic structure. According to this, mechanism the reaction is uniformly progressed on all particle surfaces. It is known that pyrite (FeS_2) exhibits a cubic crystal system, while the mechanical treatment yields particles of a spherical shape. In accordance to this and by analogy with transformation of iron disulfide to iron

monosulfide we consider that in our case of pyrite transformation to iron(II) sulfate the shrinking core equation $1 - (1- \alpha)^{1/3} = kt$ is valid.

An additional reason for this is that the established dispersion of points and coefficients are the lowest one. The rate constant determined for the time interval studied and degree of transformation up to 0.071 amounts to $K=6.434.10^{-4}$ min^{-1}.

In contrast to some cases of thermal decomposition to iron monosulfide reported in [20] mechanochemical treatment in a mill with rotating magnetic field yields iron(II) sulfate. An oxidation of S^{2-} to S^{6+} occurs in this process. The oxidation degree of iron is not changed - Fe(II). However, it is transferred from a low spin state typical for FeS_2 to a high spin state (Fe(II) into $FeSO_4$). This is evidenced by the Moessbauer parameters of hyperfine interaction (Table 1). A reaction of partial oxidation of iron sulfide to sulfate according to a shrinking core mechanism will be favored by increased concentration of structural defects in the solid, that are produced in mechanical treatment. According to the theoretical concepts for reaction kinetics in a solid [29] the appearance of the new phase nuclei on particle surface will additionally initiate the occurrence of the solid phase reaction with moving (shrinking) of the boundary between solid phases (a shrinking core mechanism). Surface analysis aiming to detection of iron sulfate species is carried out using infrared (Fig. 5) and x-ray photoelectron spectroscopy (Fig. 6).

The IR spectrum of pyrite is shown on Fig. 5. The band at 425-428 cm^{-1} corresponds to the vibration of S-S bond in pyrite, while the bands in the region 600 - 800 cm^{-1} arise due to surface oxidation of pyrite.

The IR spectra of activated samples show absorption due to HOH bonding mode at 1635 -1674 cm^{-1} and the very broad absorption at about 3400 cm^{-1} corresponding to OH^- stretching mode. These features indicate the presence of water. The non-activated sample exhibits a very little absorption at 1642 cm^{-1} and the OH^- absorption at 3572 cm^{-1} is distinct. These suggest that non-activated sample does not contain water but contains OH^-. On the pyrite surface sulfate is formed, containing OH^--$Fe(OH)SO_4$. The latter is transformed into $FeSO_4 \cdot H_2O$ at the beginning of the mechanochemical treatment and its amount is further increased.

The bond at 2950 cm^{-1} may be assigned to the C-H stretching of the -CH_2

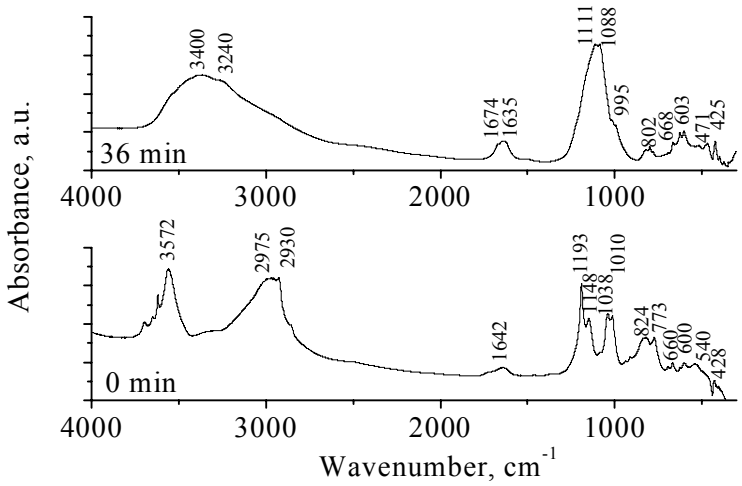

Fig. 5. IR spectra of non-activated and activated (36 min) samples

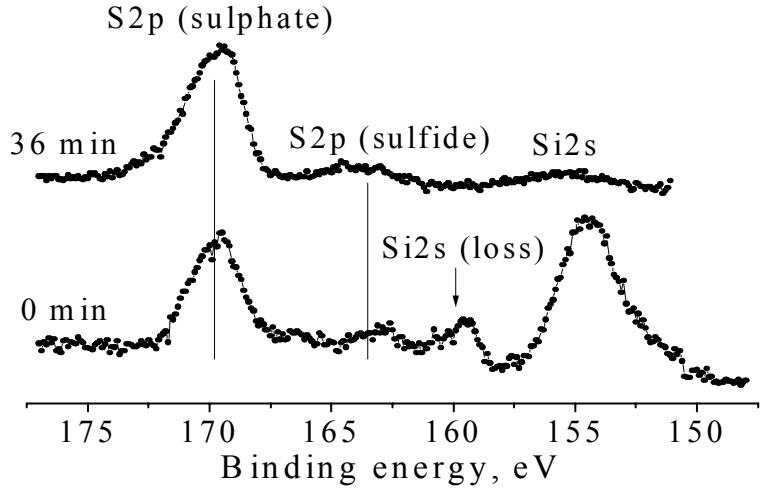

Fig. 6. XPS spectra of non-activated and activated (36 min) samples

Table 4. Surface composition of non-activated and activated 36 min samples

Sample	O, at %	Fe, at %	S, at %	Si, at %	Al, at %
0 min	66	4	5	17	8
36 min	65	17	15	3	0

groups which is registered in non activated sample (trace of flotation agent). Bands typical for $-CH_2$ group disappear in IR spectra of activated sample.

Taking into account that the characteristic frequency positions of the common sulfoxyanions are in the region 890 - 1200 cm^{-1}, the bands observed after 36 min mechanical treatment can be attributed to sulfate and thiosulfate ions [12]. The intensity of the bands at 800 cm^{-1} decreases and those at around 600 cm^{-1} increases due to mechanical treatment. The surface oxidized species are changed after mechanochemical treatment. A higher amount of sulfate is produced. The transformation of bands typical for sulfate ions is distinct. The remaining bands at 800 cm^{-1} can be due to SiO_2. The latter is present in initial pyrite but its bands overlap with that of oxidized pyrite on the surface. Results of x-ray diffraction analysis show low concentration of SiO_2. That is why it is not excluded that part of the bands in the above region can be associated with Si-O vibrations.

Iron, sulfur, oxygen and traces of carbon are present on the pyrite surface. In addition, the presence of Al and Si coming from silicates, is also observed by XPS analysis. Table 4 shows the surface composition of untreated and mechanically activated samples derived from XPS intensities.

The S2p line (Fig. 6) indicates that sulfur in the surface layers of non-activated sample is present mainly as sulfate and sulfide species. The S2p line shows that it is dominant in sulfate species (~85 at.%). The Si and Al amount decreases strongly after treating, which can be explained with exposing the bulk of the particles after grinding. Comparison of these results with data about volume content of iron sulfate derived from x-ray diffraction spectra and Moessbauer spectra reveal that only small part of sulfate sulfur is probably bonded as iron sulfate (nuclei on the surface) while the other dominating part is probably adsorbed on the surface. In accordance to high aluminum and silicon content on the surface, adsorption most probably takes place on the surface of alumina and silica.

4. Conclusions

The initial stage of pyrite transition into Fe(II) sulfate has been studied. Mechanochemical activation yields new surfaces and after interaction with oxygen a solid phase oxidation of pyrite has been achieved. The degree of oxidation of iron is preserved but iron in the resulting sulfate changes its state from low spin to high spin one. Pyrite oxidation is limited to the first step, namely to oxidation of sulfur. The energy introduced through mechanochemical activation appears to be sufficient to initiate a process not only on the surface but to yield iron sulfate in the bulk.

In the initial stage with low degree of transformation, the process obeys the kinetic of a shrinking core equation $1-(1-\alpha)^{1/3}=kt$. The reaction is of a first order. The rate constant has been determined to be $K= 6.434 \cdot 10^{-4}$ min^{-1}.

The applied spectral techniques (IR, XPS) reveal that iron sulfate nuclei are still present in the initial pyrite. In the course of mechanochemical treatment the surface is completely covered with sulfates. The transition of pyrite to sulfate in the deeper layers is limited. The transition in the bulk of pyrite crystal is strongly retarded. Its practical application needs optimization, which will be a subject of our further studies.

Acknowledgments

The authors thank the National Science Fund of the Bulgarian Ministry of Education and Science for the financial support of Projects X-1321/2003, MU-1503/2005 and to prof. Todor Peev, DSc. for helpful discussions.

References

1. J. Sammut, I. White, M.D. Melvilles, *Marine and Freshwater Research*, 47 (1996) 669.
2. K. A. Evans, C. J. Gandy, S. A. Banwart, *Mineralogical Magazine*, 67 (2003) 381.
3. M.M. Hyland, G.M. Bancroft, *Geochim. Cosmochim. Acta*, 53 (1989) 367.
4. A. Starling, J.M. Gilligan, A.H.C Carter, R.P. Foster, R.A. Saunders, *Nature*, 340 (1989) 298.
5. L.R. Hossner, J.J. Doolittle, *J. Environ. Qual*., 32 (2003) 773.
6. A.D. Brown, J.J. Jurinak, *J. Environ. Qual.*, 18 (1989) 545.

7. C.O. Moses, D.K. Nordstrom, S. Herman, A.L. Mills, *Geochim. Cosmochim. Acta*, 51 (1987) 1561.
8. B.E. Taylor, M.C. Wheeler, *Geochim. Cosmochim. Acta*, 48 (1984) 2669.
9. K.J. Edwards, T.M. Gihring, J. F. Banfield, *Appl. Environ. Microbiol.*, 65 (1999) 3627.
10. M.O. Schrenk, K. J. Edwards, R. M. Goodman, R. J. Hamers, J. F. Banfield, *Science*, 279 (1998) 1519.
11. M.N. Chandraprabha, K.A. Natarajana, P. Somasundaran, *Int. J. Miner. Process*., 75 (2005) 113.
12. M.J. Borda, D.R. Strongin, M.A. Schoonen, *Am. Mineral.*, 88 (2003) 1318.
13. N. Boyabat, A.K. Ozer, S. Bayrakceken, M.S. Gulaboglu, *Fuel Processing Technology*, 85 (2004) 179.
14. R.T Lowson, *Chem. Rev.*, 82 (1982) 462.
15. C.L. Wiersmana, J.D. Rimstidt, *Geochim. Cosmochim. Acta*, 48 (1984) 85.
16. C.O. Moses, J.S. Herman, *Geochim. Cosmochim. Acta*, 55 (1991) 471.
17. P. Chirita, Turk J. Chem., 27 (2003) 111.
18. J. P. Eymery, F. Ylli, *J. Alloys and Compounds*, 298 (2000) 306.
19. M. G. Aylmore, F.J. Lincoln, *J. Alloys and Compounds*, 242 (1996) 22.
20. E. Godocikova, P. Balaz, Z. Bastl, L. Brabec, *Appl. Surf. Sci.* 200 (2002) 36.
21. International Centre for Diffraction Data, *Alphabetical Indexes*, Pennsylvania 19073-3273, sets 1-83, 1997.
22. A.A. Temperley, H.W. Lefevre, *J. Phys. Chem. Solids*, 27 (1966) 85.
23. Th. H. de Keijser, J. I. Langford, E. J. Mittemeijer, A. B. P. Vogels, *J. Appl. Cryst.*, 15 (1982) 308.
24. S. P. Taneja ,C. N. V. Jones, *Fuel*, 63(1984) 695.
25. Huiping Hu, Quyuan Chen, Zhoulan Zhang, Jianpeng Zou, Hongsheng Che, *Thermochim. Acta*, 389 (2002) 79.
26. H. J. Shyn, P. P. Vaishnan, P. A. Montano, *Fuel,* 60 (1981) 1022.
27. R. Zboril, M. Mashlan, D. Krausova, *Czech. J. Phys.*, 51 (2001) 719.
28. D. W. Johnson, P. K. Gallager, *J. Phys. Chem*., 75(1971) 1179.
29. M. E. Brown, D. Dollimore, A. K. Galwey. Reaction in the solid state, Elsevier Sci. Publ. Company. Amsterdam-Oxford-New York, 1980 (in Russian).